of about 480 cm^{-1} in the fundamental frequency of the O_2 molecule (assuming that the $\nu_1(A_1)$ normal mode is dominated by the O–O stretching). The same effect is found by theory since the calculated $\nu_1(A_1)$ frequencies are reduced roughly 570 cm^{-1} with respect to the SCF calculated value for the fundamental frequency of O_2 ($^3\Sigma_g^-$).

The next step was to calculate the fundamental frequencies at the CI level. Unfortunately, when calculations were carried out at the distorted C_s geometries needed to calculate the second derivatives, it was found that some of these geometries were more stable than the one corresponding to the C_{2v} minimum. This fact was also observed in the RHF open-shell calculations for the allyl radical[18-21] as well as for CI calculations carried out for the HCO_2 radical.[22] This doublet instability has been examined in ref 18–22 and it was found to be due to the "shape" of the MOs obtained through RHF calculations. Inclusion of electron correlation effects by means of CI calculations is unable to recover the correct MOs and up to now it seems that the only solution comes from MC–SCF calculations.

On the other hand, it is also known[21] that the Nesbet approximation for open-shell systems often gives correctly the symmetric structure. This is probably due to the fact that this method uses a pseudo-closed-shell system with fractional occupation,[23] the final energy being corrected by adding a nonvariational term.

Thus, we have not determined the vibrational frequencies of these group 13 superoxides due to the doublet instability, but work is in progress to obtain MC-SCF results for the nonempirical pseudopotentials used here.

Conclusion

In this work, the optimized geometries and dissociation energies for the MO_2 superoxides (M = Ga, In, and Tl) have been determined at the SCF and CI levels. It is shown that these molecules have a high degree of ionic character and their molecular structures must be interpreted on the basis of both covalent and ionic valence bond states.

Vibrational frequencies calculated at the SCF level by using the Nesbet approximation[15] to treat the open shells can be summarized as follows. The $\nu_2(A_1)$ frequencies of GaO_2, InO_2, and TlO_2 are in agreement with experiment. The same holds for the $\nu_3(B_1)$ frequencies of GaO_2 and InO_2, while a discrepancy is found for TlO_2. On the other hand, a systematic deviation has been found for the $\nu_1(A_1)$ frequencies which is found to be due to the electron correlation effects.

Unfortunately, all the molecules studied here exhibit doublet instability which prohibits calculation of the fundamental frequencies at the CI level. Since this problem can generally be solved at the MC-SCF level,[22] work is now being carried out to develop an MC-SCF version of the PSHONDO-CIPSI package.

Finally, it should be pointed out that recent experimental work carried out by Sonchik et al.[24] suggests a nonsymmetrical AlOO molecule, contrary to the earlier work of Serebrennikov et al.,[25] which predicted a C_{2v} structure. A theoretical study of the AlO_2 (C_{2v}) and AlOO (C_s) molecules will be reported in a forthcoming paper.[26]

Acknowledgment. The authors thank the theoretical group of the Laboratoire de Physique Quantique de l'Université Paul Sabatier de Toulouse, France, for making available the computer programs used here as well as details concerning the pseudopotentials and basis sets. The calculations were carried out on the IBM 3083 computer at the Centre de Câlcul de la Universitat de Barcelona and its financial support is gratefully acknowledged.

Registry No. GaO_2, 51199-55-4; InO_2, 12600-43-0; TlO_2, 67657-12-9.

(18) Mc Kelvey, J. M.; Berthier, G. *Chem. Phys. Lett.* **1976**, *41*, 476.
(19) Paldus, J.; Veillard, A. *Mol. Phys.* **1978**, *35*, 445.
(20) Kikuchi, O. *Chem. Phys. Lett.*, **1980**, *72*, 487.
(21) Baird, N. C.; Gupta, R. R.; Taylor, K. F. *J. Am. Chem. Soc.* **1979**, *101*, 4531.
(22) Ellinger, Y. "Abstract's Book of the XVth Meeting of Theoretical Chemists of Latin Expression", Comm. C-22. Mc Lean, A. D.; Elllinger, Y. *Chem. Phys. Lett.* **1983**, *98*, 450.
(23) Olivella, S., private communication.
(24) Sonchik, S. M.; Andrews, L.; Carlson, K. D. *J. Phys. Chem.* **1983**, *87*, 2004.
(25) Serebrennikov, L. V.; Osin, S. B.; Maltsev, A. A. *J. Mol. Struct.* **1982**, *81*, 25.
(26) Cabot, P. L1.; Illas, F.; Ricart, J. M.; Rubio, J., work in progress.
(27) The group notation is being changed in accord with recent actions by IUPAC and ACS nomenclature committees. A and B notation is being eliminated because of wide confusion. Group I becomes groups 1 and 11, group II becomes groups 2 and 12, group III becomes groups 3 and 13, etc.

Theoretical Determination of Molecular Structure and Conformation. 17. On the Existence of FH_2^-, OH_3^-, NH_4^-, and CH_5^- in the Gas Phase

Dieter Cremer* and Elfi Kraka

Lehrstuhl für Theoretische Chemie, Universität Köln, D-5000 Köln 41, West Germany
(Received: May 31, 1985)

Ab initio calculations (HF/6-31G* and MP2/6-31++G**) carried out for FH_2^-, OH_3^-, NH_4^-, and CH_5^- indicate that these ions are most stable in the form of AH_n-solvated H^- ions. Theoretical binding energies (42, 26, 15, and 6 kcal/mol) decrease with decreasing polarity of the AH bond. Apart from CH_5^-, all $H^-\cdot AH_n$ complexes can rearrange via internal proton transfer to $AH_{n-1}^-\cdot H_2$ complexes which are 2–15 kcal/mol less stable than the former. Investigation of the various dissociation channels of AH_{n+1}^- ions reveals that NH_4^-, OH_3^-, and FH_2^- are sufficiently stable in the gas phase to be detected by mass spectrometry.

I. Introduction

Recent investigations by Nibbering and co-workers[1-3] have provided convincing evidence that H_3O^- and NH_4^- are relatively long-lived species in the gas phase.[4] They can be generated in a Fourier-transform ion cyclotron resonance mass spectrometer by oxidation of formaldehyde with OH^- and NH_2^-, respectively. The first step in the formation of the electron-rich hydrides most probably involves a collision complex between the ion AH_{n-1}^-

(1) Kleingeld, J. C.; Nibbering, N. M. M. *Int. J. Mass. Spectrom. Ion Phys.* **1983**, *49*, 311–318.
(2) Kleingeld, J. C. Ph.D. Thesis, Amsterdam, 1983.
(3) Kleingeld, J. C.; Ingemann, S.; Jalonen, J. E.; Nibbering, N. M. M. *J. Am. Chem. Soc.* **1983**, *105*, 2474–2475.
(4) For an independent conformation of the existence of H_3O^- by an ion-beam experiment, see Paulson, J. F.; Henchman, M. J. *Bull. Am. Phys. Soc.* **1982**, *27*, 108.

0022-3654/86/2090-0033$01.50/0

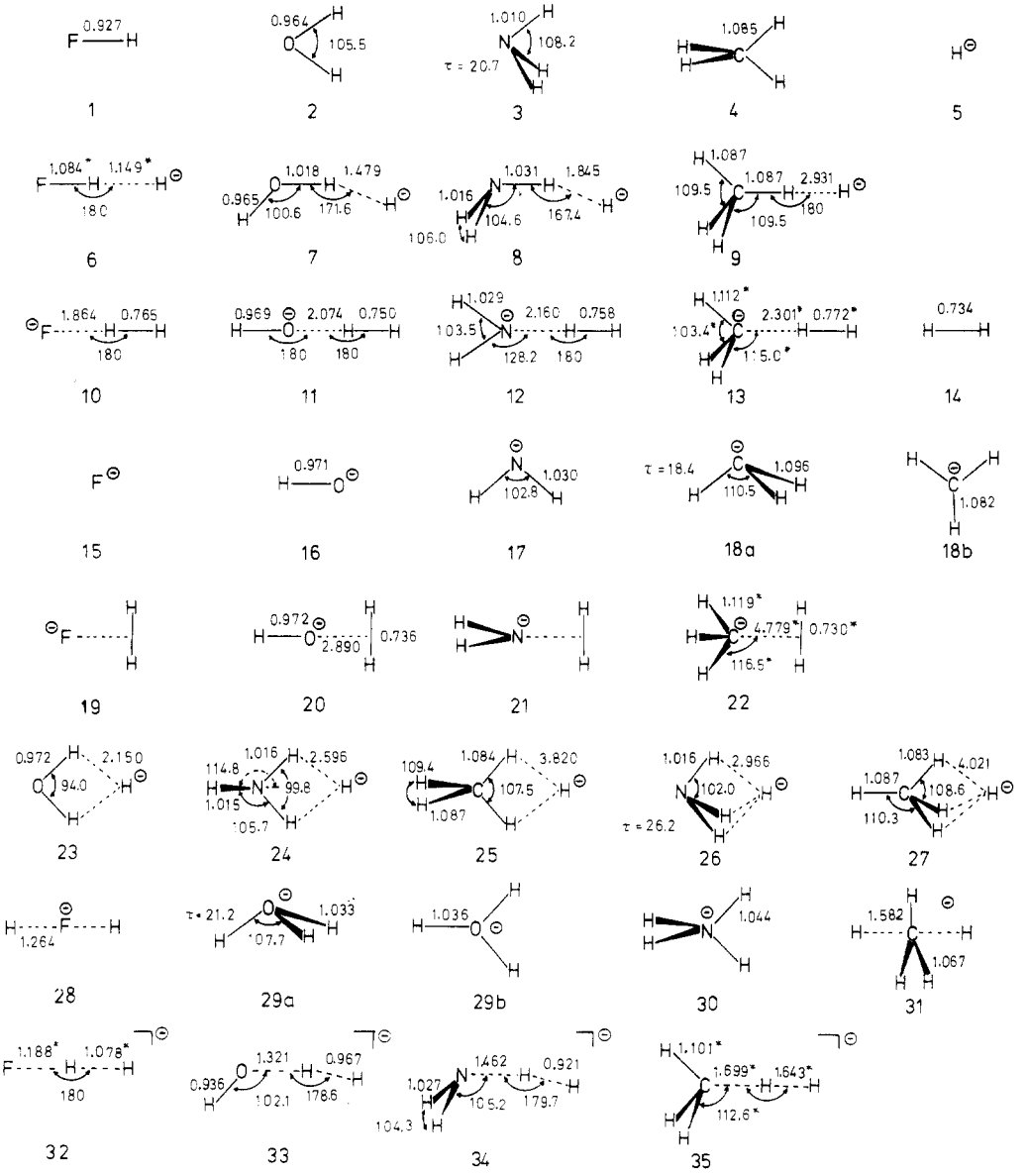

Figure 1. MP2/6-31++G** geometries of **1–31**. **32–35** correspond to calculated transition-state geometries of proton-transfer reaction 2. Starred values denote HF/6-31G* values. The angle τ determines the degree of nonpolarity for pyramidal molecules.

(OH^-, NH_2^-) and the neutral which then decomposes by successive proton and hydride transfer to carbon monoxide and AH_{n+1}^- (H_3O^-, NH_4^-):[1-3]

$$AH_{n-1}^- + H_2CO \rightleftharpoons [AH_{n-1}^- \cdots H_2CO] \rightleftharpoons [AH_n \cdots HCO^-] \rightarrow \rightarrow AH_{n+1}^- + CO \quad (1)$$

The hydride transfer occurs either in the complex $AH_n \cdots HCO^-$ (A = O) or after its decomposition (A = N). Deuterium-labeling experiments indicate that the hydrogen atoms of H_3O^- and NH_4^- are not equivalent. Therefore, their structure has been described as a hydride ion solvated by a water or an ammonia molecule.[1-3]

Stimulated by these fascinating observations we have carried out ab initio calculations in order to investigate the association between molecules AH_n for A = F, O, N, C (**1–4**, Figure 1) and an H^- ion (**5**). Association can lead to a type I AH_{n+1}^- complex shown in Scheme I (see also Figure 1, **6–9**). Type I complexes may rearrange to type II complexes (Figure 1, **10–13**) which are composed of H_2 (**14**) and anions AH_{n-1}^- **15–18**. Thus complexes I and II can be considered as possible intermediates of the proton-transfer reaction

$$AH_n + H^- \rightarrow AH_{n-1}^- + H_2 \quad (2)$$

Accordingly, a theoretical investigation of complexes AH_{n+1}^- inevitably entails an exploration of the potential energy surface of reaction 2.

A priori it is difficult to say whether a solvated H^- is more stabilized in complex I or in the bifurcated structure of complex III (Scheme I and **23–25** in Figure 1), which has been suggested by Nibbering and co-workers for H_3O^-.[1,2] If $n \geq 3$, the AH_n molecule may even direct three AH bonds at an approaching H^- ion thus leading to the trifurcated structure IV of scheme I (**26**, **27**, Figure 1). An alternative to complex II is the T-shaped complex V (Scheme I and **19–22** in Figure 1) with both hydrogens of H_2 being at equal or similar distance from the negatively charged atom A. Finally, one can consider structures with the H^- ion approaching AH_n (A = F, O, N) on its electron lone pair side. It is easy to see that these structures are highly destabilized due to electron pair–electron pair repulsion. If, however, the incoming H^- ion possesses sufficient energy, the highly symmetrical structure VI of Scheme I (**28–31**, Figure 1) can be adopted. In case of A = F or C, VI corresponds to the transition state (TS) of the S_N2 reaction

$$H^- + AH_{n-1}H \rightarrow HAH_{n-1} + H^- \quad (3)$$

In order to give an account of the relative stability of complexes I–VI, we have determined the equilibrium geometries, energies, and charge distributions of **1–31** (Figure 1). On the basis of the analysis of these data the following questions are answered in this work: (1) What does the energy profile of proton transfer reaction 2 look like? (2) Which of the possible ion–neutral complexes is

SCHEME I

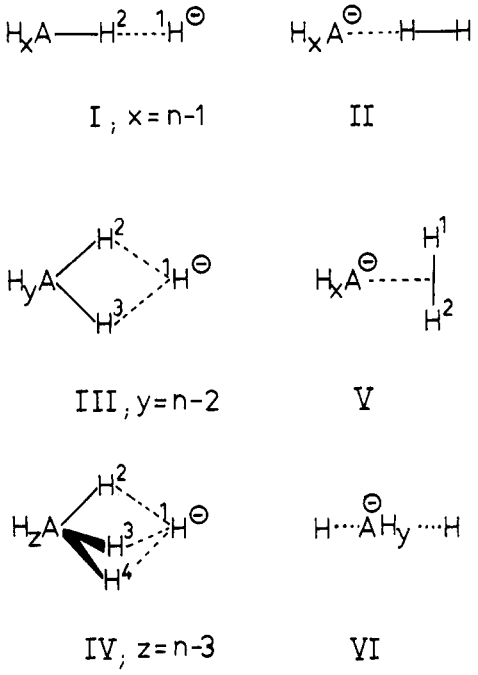

actually observed in experiment? (3) Does there exist a long-lived ion–neutral complex CH_5^- or FH_2^-? (4) What are the forces dominating the stability of complexes AH_{n+1}^-?

Before representing our results it is interesting to note that some of these questions have been dealt with already 20 years ago by Ritchie and King.[5] In three pioneering ab initio studies on proton-transfer reactions these authors calculated the minimum energy path of (2) for A = H, F, O, N, and C with basis sets including already flat s,p functions in order to correctly describe the tail behavior of the anion MOs. Although their final results differ from ours, partially due to incomplete optimization and partially due to the difficulty of getting reliable estimates of correlation energies in the mid-sixties, their calculated energy profiles are in qualitative accord with ours.

Apart from this early work only scattered theoretical investigations on AH_{n+1}^- (A = F, O, N, C) ions can be found in the literature. Most of them consider the transition state of the S_N2 reaction between CH_4 and H^-.[6] Kari and Csizmadia have calculated D_{3h}-symmetrical H_3O^- at the Hartree–Fock level employing a DZ+P basis set.[7] They find H_3O^- to be unstable by 99 kcal/mol relative to the dissociation products H_2O and H^-. A much lower value of about 30 kcal/mol has been calculated by Glidewell at the semiempirical MINDO/3 level.[8] However, both studies show that D_{3h}-symmetrical H_3O^- (and, in the same way, T_d-symmetrical NH_4^-[8] is a highly unstable species. Recently, an extensive investigation of H^- migration in NH_4^- has been published by Kalcher, Rosmus, and Quack.[9] These authors employed a [7s4p1d/4s] basis augmented by diffuse sp functions. Their SCEP-CEPA results are in qualitative agreement with those presented in this work.

II. Numerical Methods

In order to get a reliable description of the energy profile of reaction 2, two basic requirements have to be fulfilled: (a) The description of the system $AH_n + H^-$ has to be consistent with that of $AH_{n-1}^- + H_2$ for a variation of A from C to F. (b) Since the complexes investigated are held together predominantly by electrostatic forces, charge distribution and charge polarization have to be evaluated rather accurately. A priori one would expect that both requirements are met only if basis sets of at least DZ quality augmented by polarization functions and sets of diffuse s,p Gaussian-type functions (GTF) are used. However, by testing a variety of basis sets we found that Pople's 6-31G* basis[10] already provides a reasonable account of the energy profile of reaction 2. This has to do with the fact that relative proton affinities (PA) of **5** and **15–18** are satisfactorily determined with the 6-31G* basis at the Hartree–Fock level (HF/6-31G*) although absolute PA values are far too large (~40 kcal/mol) at this level of theory. Taking advantage of this, we have optimized the geometries of complexes I–VI first at the HF/6-31G* level. In the next step we have introduced one set of flat s,p GTFs which is essential for the description of diffuse electron distributions typical of anions.[5,6,11,12] Exponents of the diffuse s,p shell ($\alpha_s = \alpha_p$) have been taken from Clark et al.[12c] who recommend just one flat s GTF in the case of the H^- ion. These authors have termed such a basis set 6-31++G**. Apart from the 6-31++G** basis we have also employed basis sets with diffuse p functions at H in order to improve the description of charge polarization in an H_2 molecule approached by an anion. The corresponding geometries and relative energies differ, however, only slightly from those obtained with the 6-31++G** basis. AH bond lengths are underestimated at the HF/6-31G* and HF/6-31++G** level. At the same time their polar character is overestimated yielding H atoms which are charged too positively. As a consequence, electrostatic H,H interactions and, hence, binding energies of solvated H^- ions are also overestimated at this level of theory. Consideration of correlation corrections reverts this trend. For example, application of second-order Møller–Plesset (MP2) perturbation theory[13] leads to AH bond lengths somewhat longer than experimental values.[14,15] Accordingly, electrostatic interactions and binding energies of AH_{n+1}^- complexes are underestimated at the MP2 level. In view of these trends we have reoptimized all molecular geometries considered in this work at the MP2/6-31++G** level of theory in order to get upper bounds to AH bond distances and lower bounds to true binding energies of complexes AH_{n+1}^-. The location of the transition state of reaction 2 has been determined by increasing $R(A,H^2)$ of I stepwise and optimizing all remaining parameters. The maximum of the resultant energy curve $E(R)$ has been evaluated by applying simple interpolation techniques and by reoptimizing the transition-state geometry for the corresponding $R(A,H^2)$ value.

III. Results and Discussion

In Figure 1 optimized MP2/6-31++G** geometries are depicted. In those cases (**6**, **9**, **22**) where no equilibrium geometries have been found at this level of theory, HF/6-31G* parameters are given (for other HF/6-31G* geometries see Table I).

(5) (a) Ritchie, C. D.; King, H. F. *J. Am. Chem. Soc.* **1966**, *88*, 1069–1070. (b) Ritchie, C. D.; King, H. F. *J. Am. Chem. Soc.* **1968**, *90*, 825–833, 833–838, 838–843.

(6) (a) Peyerimhoff, S. D.; Römelt, J. *Phys. Bl.* **1984**, *40*, 300–304. (b) Ishida, K.; Morokuma, K.; Komornicki, A. *J. Chem. Phys.* **1977**, *66*, 2153–2156. (c) Keil, F.; Ahlrichs, R. *J. Am. Chem. Soc.* **1976**, *98*, 4787–4793. (d) Baybutt, P. *Mol. Phys.* **1975**, *29*, 389–403. (e) Dyczmons, V.; Kutzelnigg, W. *Theor. Chim. Acta* **1974**, *33*, 239–247. (f) Dedieu, A.; Veillard, A.; Roos, B. In "Chemical and Biochemical Reactivity", The Jerusalem Symposium on Quantum Chemistry and Biochemistry; Reidel: Boston, 1974; pp 371–375. (g) Dedieu, A.; Veillard, A. *J. Am. Chem. Soc.* **1972**, *94*, 6730–6738. (h) Mulder, J. J. C.; Wright, J. S. *Chem. Phys. Lett.* **1970**, *5*, 445–449.

(7) Kari, R. E.; Csizmadia, I. G. *J. Am. Chem. Soc.* **1977**, *99*, 4539–4545.

(8) Glidewell, C. *J. Mol. Struct.* **1980**, *67*, 121–132.

(9) Kalcher, J.; Rosmus, P.; Quack, M. *Can. J. Phys.* **1984**, *62*, 1323–1327.

(10) Hariharan, P. C.; Pople, J. A. *Theor. Chim. Acta* **1973**, *28*, 213–222.

(11) See, e.g., (a) Duke, A. J. *Chem. Phys. Lett.* **1973**, *21*, 275–282. (b) Ahlrichs, R. *Chem. Phys. Lett.* **1973**, *18*, 521–524. (c) Webster, B. *J. Phys. Chem.* **1975**, *79*, 2809–2814. (d) Dunning, T. H.; Hay, P. J. *Mod. Theor. Chem.* **1977**, *3*, 1–27.

(12) (a) Chandrasekhar, J.; Andrade, J. G.; Schleyer, P. v. R. *J. Am. Chem. Soc.* **1981**, *103*, 5609–5612. (b) Spitznagel, G. W.; Clark, T.; Chandrasekhar, J.; Schleyer, P. v. R. *J. Comp. Chem.* **1982**, *3*, 363–371. (c) Clark, T.; Chandrasekhar, J.; Spitznagel, G. W.; Schleyer, P. v. R. *J. Comp. Chem.* **1983**, *4*, 294–301.

(13) (a) Møller, C.; Plesset, M. S. *Phys. Rev.* **1934**, *46*, 618–622. (b) Pople, J. A.; Binkley, S.; Seeger, R. *Int. J. Quantum Chem. Symp.* **1976**, *10*, 1–19.

(14) Cremer, D. *J. Chem. Phys.* **1978**, *69*, 4440–4455, 4456–4471.

(15) DeFrees, D. J.; Levi, B. A.; Pollack, S. K.; Hehre, W. J.; Binkley, J. S.; Pople, J. A. *J. Am. Chem. Soc.* **1979**, *101*, 4085–4089.

TABLE I: Calculated HF/6-31G* Energies and Geometries of Complexes I and II

complex	energy, hartree	geometry (R, Å; ∠, ϕ deg)
6	−100.497 99	$R(H^1H^2)$ = 1.149; $R(FH^2)$ = 1.084; ∠FHH = 180
7	−76.480 76	$R(H^1H^2)$ = 1.508; $R(OH^2)$ = 1.014; $R(OH^3)$ = 0.949; $\angle H^1H^2O$ = 169.8; $\angle H^2OH^3$ = 99.9
8	−56.636 21	$R(H^1H^2)$ = 1.776; $R(NH^2)$ = 1.042; $R(NH^3)$ = 1.008; $R(NH^4)$ = 1.009; $\angle H^1H^2N$ = 168.7; $\angle H^2NH^3$ = 103.1; $\angle H^2NH^4$ = 103.1; $\angle H^3NH^4$ = 104.1; $\phi(H^1H^2NH^3)$ = 54.1
9	−40.631 13	$R(H^1H^2)$ = 2.215; $R(CH^2)$ = 1.097; $R(CH^3)$ = 1.089; $\angle H^1H^2C$ = 180; $\angle H^2CH^3$ = 110.2
10	−100.499 94	$R(H^1H^2)$ = 0.802; $R(FH^2)$ = 1.607; ∠FHH = 180
11	−76.472 28	$R(H^1H^2)$ = 0.803; $R(OH^2)$ = 1.719; $R(OH^3)$ = 0.957; $\angle H^1H^2O$ = 180; $\angle H^2OH^3$ = 97.2
12	−56.618 28	$R(H^1H^2)$ = 0.790; $R(NH^2)$ = 1.953; $R(NH^3)$ = 1.025; $\angle H^1H^2N$ = 180; $\angle H^2N(H^3H^4)$ = 101.0; $\angle H^3NH^4$ = 100.0
13	−40.608 05	$R(H^1H^2)$ = 0.772; $R(CH^2)$ = 2.301; $R(CH^3)$ = 1.112; $\angle H^1H^2C$ = 180; $\angle H^2CH^3$ = 115.0; $\angle H^3CH^4$ = 103.4
32	−100.497 77	$R(H^1H^2)$ = 1.078; $R(FH^2)$ = 1.188; ∠FHH = 180
33	−76.470 96	$R(H^1H^2)$ = 1.147; $R(OH^2)$ = 1.368; $R(OH^3)$ = 0.952; $\angle H^2OH^3$ = 99.4
34	−56.616 39	$R(H^1H^2)$ = 1.184; $R(NH^2)$ = 1.589; $R(NH^3)$ = 1.032; $\angle H^2NH^3$ = 100.1; $\angle H^3NH^4$ = 101.8
35	−40.602 16	$R(H^1H^2)$ = 1.643; $R(CH^2)$ = 1.699; $R(CH^3)$ = 1.101; $\angle H^2CH^3$ = 112.6

TABLE II: Calculated Absolute Energies and Correlation Energies[a]

molecule	HF/6-31G*// HF/6-31G*	MP2/6-31++G**//MP2/6-31++G** absolute	correlation
FH (**1**)	−100.002 91	−100.218 30	−0.194 76
OH_2 (**2**)	−76.010 75	−76.236 21	−0.205 81
NH_3 (**3**)	−56.184 34	−56.396 33	−0.195 46
CH_4 (**4**)	−40.195 17	−40.371 43	−0.169 26
H^- (**5**)	−0.422 44	−0.503 63	−0.016 55
$FH\cdots H^-$ (**6**)	−100.497 99	−100.792 35[b]	−0.234 60
$OH_2\cdots H^-$ (**7**)	−76.480 76	−76.769 64	−0.232 73
$NH_3\cdots H^-$ (**8**)	−56.636 21	−56.914 40	−0.217 88
$CH_4\cdots H^-$ (**9**)	−40.631 13	−40.877 83	−0.187 08
H_2 (**14**)	−1.126 83	−1.157 77	−0.026 37
F^- (**15**)	−99.350 48	−99.626 07	−0.207 48
OH^- (**16**)	−75.326 60	−75.605 31	−0.221 64
NH_2^- (**17**)	−55.476 08	−55.735 52	−0.208 13
CH_3^- (**18a**)	−39.466 79	−39.686 90	−0.176 37
CH_3^- (**18b**)	−39.446 16	−39.683 12	−0.176 68

[a] All values in hartree. [b] Energy of complex **10** is given.

TABLE III: Theoretical Energies and Experimental Enthalpies of the Proton-Transfer Reaction $AH_n + H^- \rightarrow AH_{n-1} + H_2$[a]

A	exptl PA[b]	exptl ΔH_R[b]	HF/6-31G*// HF/6-31G* ΔE_R	HF/6-31G*// HF/6-31G* σ	MP2/6-31++G**//MP2/6-31++G** ΔE_R	MP2/6-31++G**//MP2/6-31++G** σ
C	416.6	16.2	15.1	−1.1	19.1	2.9
N	403.6	3.2	2.4	−0.8	4.2	1.0
O	390.8	−9.6	−12.7	−3.1	−14.6	−5.0
F	371.3	−29.1	−32.6	−3.5	−38.9	−9.8

[a] All values in kcal/mol. σ denotes the deviation of theoretical ΔE_R values from experimental ΔH_R values. [b] $\Delta H_R = PA(AH_{n-1}^-) - PA(H^-)$. The proton affinity of H^- is 400.4 kcal/mol. Reference 33.

Calculated absolute and relative energies are summarized in Tables II (HF and MP2 energies), III (energies ΔE_R of the proton-transfer reaction 2), IV (relative energies of complexes I and II), and V (relative energies of complexes III–VI).

Geometries. The following trends become obvious by inspection of the data of Figure 1. (1) In type I complexes atoms A, H^2, and H^1 are in a linear or an almost linear arrangement which is in line with the results obtained by Ritchie and King.[5,6] The distance $R(H^1,H^2)$ decreases from C to F. At the same time the bond length $R(A,H^2)$ increases relative to that in the free AH_n molecule by 0.002 (A = C), 0.021 (N), 0.054 (O), and 0.157 Å (F). Hydrogen atom H^2 is pulled toward the H^- ion the more polar the AH^2 bond becomes. This trend has to do with the electron-acceptor ability of A and is contrary to the A–H bond strength.[16] At the MP2/6–31++G** level the HF molecule looses a proton without barrier upon H^- approach while at the HF/6-31G* level **6** represents a local minimum of the FH_2^- energy surface. In **7** and **8** the HAH angles are smaller than in **2** and **3** which is probably due to electrostatic attraction between H^- and the more distant H^3 (H^4) atom(s).

(2) In type II complexes changes of the geometrical parameters for a variation of A from F to C are less regular. If appropriate levels of theory are compared, the nonbonded distance $R(A,H^2)$ is 0.1–0.6 Å larger than $R(H^1,H^2)$ in I. The bond distance $R(H^1,H^2)$ is slightly lengthened by 0.016–0.024 Å. Somewhat unexpected **10**, **11**, and **12** adopt highly symmetrical geometries, namely, $C_{\infty v}$ (**10**, **11**) and C_{2v} (**12**). However, the potential energy surface is rather flat in the direction of H^3AH^2 bending. An energy increase < 0.6 kcal/mol has the H_2 (AH_{n-1}^-) molecule swinging back and forth by more than 50°, e.g.

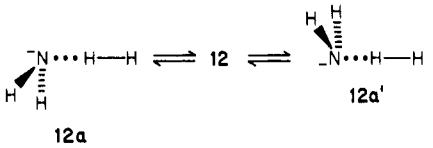

At the HF/6-31G* level, **11a** and **12a** are more stable than **11** and **12**, probably due to significantly shorter $R(A,H^2)$ distances.

(3) In type III and type IV complexes the same dependence of nonbonded distances $R(H^1,H^2)$, etc. on the polarity of the AH bond is found as in I. Again, the H^2AH^3 angles are smaller than in the free AH_n molecules. In this way electrostatic attraction between H^- and the positively charged H^3, H^4, etc. atoms is increased.

(4) Type V complexes contain essentially nondeformed AH_{n-1}^- and H_2 molecules which seem to associate rather loosely at distances of 3–4 Å. **19** and **21** were found only when the H basis was augmented with flat p functions.

(5) Highly symmetrical arrangements of the H atoms around A lead to considerable lengthening of AH distances which are largest for those structures corresponding to the transition states of a S_N2 reaction (**28**, **31**). Contrary to previous results[8,9] our calculations suggest that OH_3^- (**29**) prefers a pyramidal (C_{3v}) rather than a planar (D_{3h}) geometry (E(**29b**) − E(**29a**) = 3.4 kcal/mol).

Energies. Energies ΔE_R of the proton-transfer reaction 2 are a measure of the relative proton affinity (PA) of **15**–**18** using H^- as a reference:

$$\Delta H_R = PA(AH_{n-1}^-) - PA(H^-) \approx \Delta E_R$$

Three situations can be distinguished (Figure 2a–c): (a) For anions AH_{n-1}^- (neutrals AH_n) with a larger PA value (lower acidity) proton-transfer reaction 2 is endothermic (ΔH_R, $\Delta E_R > 0$); (b) for anions with comparable PA values reaction 2 is thermoneutral (ΔH_R, $\Delta E_R \approx 0$); (c) for anions (neutrals) with lower PA values (larger acidity) reaction 2 is exothermic (ΔH_R, $\Delta E_R < 0$). According to the experimental PA and ΔH_R values listed in Table III situation (a) applies to A = C, situation (b) to A = N although the reaction is slightly endothermic (by 3 kcal/mol), and situation (c) to A = O and F.

(16) Stull, D. R., Prophet, H., Ed., "JANAF Thermochemical Tables", *Natl. Stand. Ref. Data Ser., Natl. Bur. Stand.* **1974**, *No. 37*. $DH°_{298}(F-H)$ = 136.1; $DH°_{298}(OH-H)$ = 119.3; $DH°_{298}(H_2N-H)$ = 103.2; $DH°_{298}(H_3C-H)$ = 104.8 kcal/mol.

TABLE IV: Relative Energies of Complexes I and II and Intrinsic Barriers to Proton Transfer[a]

	HF/6-31G*//HF/6-31G*				MP2/6-31++G**/MP2/6-31++G**				estimated values[c]			
C	ΔE_I	ΔE_{II}	ΔE_{II-I}[b]	E_a[b]	ΔE_I	ΔE_{II}	ΔE_{II-I}[b]	E_a[b]	ΔE_I	ΔE_{II}	ΔE_{II-I}	stability[d]
C	−8.5	−9.0	15.7	10.8	−1.7				−6	−7	15	6
N	−18.5	−9.6	12.1	13.3	−9.1	−4.6	7.7	10.4	−15	−8	10	15
O	−29.9	−11.8	8.5	9.2	−18.7	−4.8	4.3	7.0	−26	−9	7	16
F	−45.6	−14.2	2.3	3.6		−5.3			−42	−11	2	13

[a] For a definition of energy differences compare with Figure 2. All energies in kcal/mol. [b] Corrected for errors in calculated PA values. See Table III. E_a values have also been corrected to fix differences $E_a - E_{II-I}$ at calculated values. [d] Stability of the $H^-{\cdot}AH_n$ complex given with regard to most stable dissociation products.

TABLE V: Relative Energies (MP2/6-31++G//MP2/6-31++G**) of Type III, IV, V, and VI Complexes with regard to Dissociation Products[a]**

A	III, bifurcated		IV, trifurcated		V, T-shaped		VI	
F					**19**	0	**28**	37.9
O	**23**	−15.2 (3.5)			**20**	−0.3	**29a**	21.1
							29b	24.5
N	**24**	−6.7 (2.3)	**26**	−6.6 (2.4)	**21**	0	**30**	1.3
C	**25**	−0.6 (1.1)	**27**	−0.5 (1.2)	**22**	0	**31**	54.5

[a] Compare with Scheme I and Figure 1. All values in kcal/mol. Numbers in parentheses are energies relative to type I complexes. Energies of type VI complexes relative to $AH_n + H^-$.

HF/6-31G* energies reproduce experimental ΔH_R values satisfactorily (mean deviation $\bar{\sigma}$ = 2.1 kcal/mol) due to a consistent description of PAs. The value of $\bar{\sigma}$ is twice as large for MP2/6-31++G** energies. At both levels of theory deviations σ become more negative for a variation of A from C to F. This is a result of decreasing n in AH_n and AH_{n-1}^-, respectively.[17] Similar errors are involved in calculated energy differences ΔE_{II-I} between type I and type II complexes (Figure 2). In order to take this into account all calculated ΔE_{II-I} values are corrected by the appropriate σ values of Table III.

Theoretical energy differences ΔE_I, ΔE_{II}, and ΔE_{II-I} (Table IV) reveal that in all cases considered type I complexes are more stable than type II complexes. However, ΔE_{II-I} becomes relatively small when going from A = C to A = F. In the latter case, **6** and **10** probably possess similar energies with **6** being slightly more stable. Type III and type IV complexes are only 1–3 kcal/mol less stable than type I complexes (Table V). They correspond to transient points of a H^- ion rapidly moving on the hydrogen "face" of an AH_n molecule

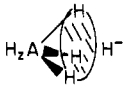

between the most favorable positions close to H^2, H^3, etc. Contrary to I–IV, the binding energy of type V complexes (relatively to the dissociated products) is vanishingly small. Thus, they will not play any significant role in a collision-induced proton transfer.

As expected type VI structures **28**, **29**, and **31** possess rather high energies. Surprisingly, this does not hold for T_d-symmetrical NH_4^- (**30**), which is only 1.3 kcal/mol less stable than $NH_3 + H^-$ (Table V). Analysis of results reveals that this is not an artifact of the theoretical methods used. For example, the relative energy of the transition state **31** of the nucleophilic displacement reaction 3 for A = C (54.5 kcal/mol, Table V) is in excellent agreement with elaborate CI and CEPA calculations.[6] Also, the lower relative energy of **28** is in line with the fact that the electronegative F atom can accept negative charge better than a C atom. In **29**, negative charge is distributed over four rather than three atoms as in **28**

(17) This has to do with the fact that at a given basis set level a spherical F^- ion is easier to describe than linear F–H, linear OH^- in turn easier than bent H_2O, and nearly "spherical" CH_4 easier than pyramidal CH_3^-. For NH_2^- and NH_3 the same basis set errors can be expected thus yielding the lowest σ values.

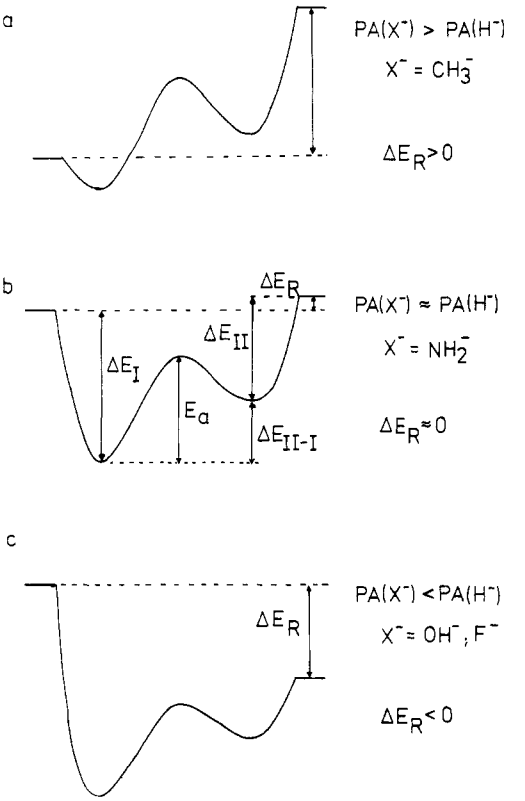

Figure 2. Energy profile of reaction 2 for an (a) endothermic, (b) thermoneutral, and (c) exothermic proton transfer.

and **31**. A further decrease in relative energy is calculated (Table V). Hence, the relatively low energy of **30** can be considered as being the result of charge distribution to five atoms. Since negative charge resides in the σ^*(AH) MOs, elongation of AH bonds in **28–31** (0.337, 0.069, 0.034, and 0.497 Å) relative to those of parent compounds **1–4** (Figure 1) is a good indicator of the extent of charge distribution and the resultant relative energy.

On the basis of the energies given in Tables IV and V it can be concluded that it is sufficient to consider just type I and type II complexes as intermediates of the proton-transfer reaction 2. All relevant energy parameters needed to construct the energy diagrams of Figure 2 are given in Table IV. Calculated E_a barriers (Figure 2) have been corrected by σ values in the same way as ΔE_{II-I} differences. Apart from A = C, the calculated intrinsic barriers E_a for proton transfer are all smaller than the solvation energy ΔE_I of an H^- ion. If **6**, **7**, or **8** are formed from AH_n and H^-, they will possess sufficient energy to surmount the central barrier and rearrange to the H_2-solvated anions AH_{n-1}^-. This process can be facilitated by proton tunneling through the central barrier.

For A = O and F the excess energy of type I complexes suffices to overcome even the binding energy of type II complexes, ΔE_{II}, and to yield as dissociation products H_2 and AH_{n-1}^-.

Charge Distribution and Binding Forces. In the gas phase an ion and a neutral molecule attract each other by long-range ion–dipole and ion–induced dipole forces. For neutrals possessing a dipole moment of 1.5–2 D, these forces become larger than RT at distances r of 14–15 Å while for nonpolar molecules like H_2

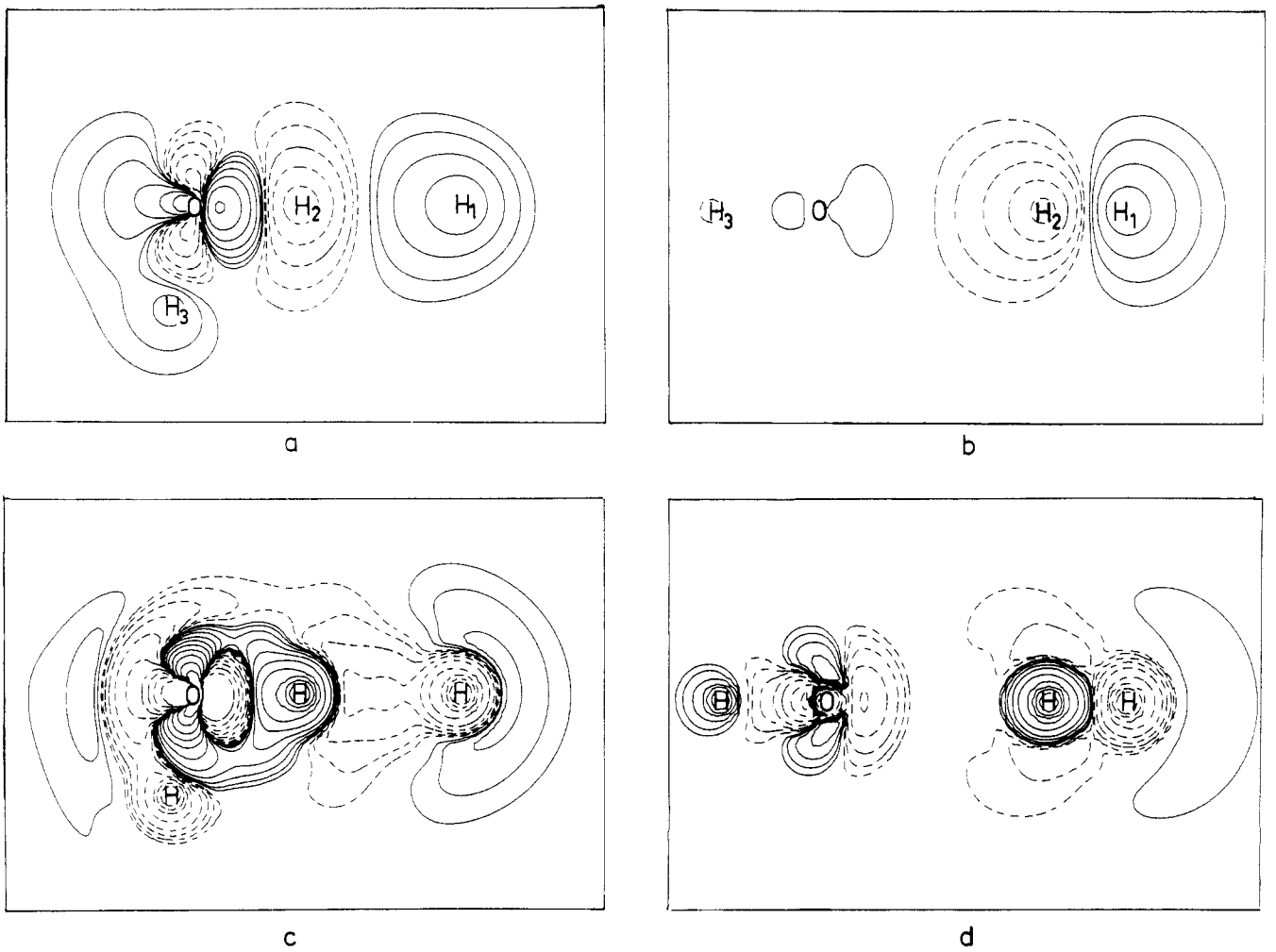

Figure 3. Calculated difference electron density distributions $\Delta\rho(\mathbf{r})$ (e/Å^3) for H_3O^- complexes **7** (a) and **11** (b). Parts c and d show the corresponding difference concentration distributions $\Delta(\nabla^2\rho(\mathbf{r}))$ (e/Å^5). Dashed (solid) contour lines correspond to negative (positive) $\Delta\rho(\mathbf{r})$ values. In the case of $\Delta(\nabla^2\rho(\mathbf{r}))$ they indicate charge concentration (depletion).

this level of attraction is achieved at r = 4–5 Å.[18] Nonclassical interactions between ion and neutral become important in the same measure as the wave functions of the two closed-shell species overlap. There are possible stabilizing charge-transfer interactions and destabilizing overlap repulsion. In addition, the ion and the molecule can change their geometries as to maximize all stabilizing forces (polarization, charge transfer, dispersion).

In order to make an assessment of the various interactions in complexes **6–13**, we have calculated atomic monopole (charges), dipole, and quadrupole moments employing the virial partitioning method.[19] Contrary to the Mulliken population analysis, this method provides reasonable gross atomic charges even when basis sets with diffuse GTF's are used.[20] By comparison of calculated virial charges with the corresponding values of the noninteracting closed-shell species, we have quantitatively determined the amount of charge transferred and the degree of charge polarization. According to these results, which will be published in more detail elswhere,[21] charge transfer from ion to neutral or vide versa is negligible amounting to just a few millielectrons.[20] On the other hand, charge polarization is considerable, accounting for most of the binding energy of type II complexes.

The degree of charge polarization can also be assessed by inspection of the difference electron density distributions[22]

$$\Delta\rho(\mathbf{r}) = \rho(\mathbf{r})^{\text{complex}} - \rho(\mathbf{r})^{\text{procomplex}}$$

which reflect the change in $\rho(\mathbf{r})$ upon complex formation. In Figure 3 contour line diagrams of $\Delta\rho(\mathbf{r})$ are shown for H_3O^- complexes **7** and **11**. In the case of **7** (Figure 3a) the charge of the incoming H^- ion contracts and pushes the electron density from H^2 toward the O atom where it builds up in front of the nucleus. There is a decrease of electron density in the bond OH^3 coupled with an increase of $\rho(\mathbf{r})$ at the position of nucleus H^3. Thus, the density pattern of complex **7** reveals alternating changes in ρ along the atom chain H^1, H^2, O, and H^3. This is equivalent to a charge transfer within the H_2O molecule from H^2 toward H^3, which increases the electrostatic attraction between ion and molecule. Figure 3a contains also information about the possible fate of **7** in a collision reaction. According to $\Delta\rho(\mathbf{r})$, there will be a heterolytic cleavage of the OH^2 bond and the formation of an oxygen lone pair, which will polarize the newly formed HH bond. Atom H^3 will swing into the axis H^1H^2O where there is a significant accumulation of electron density behind the O nucleus.

Figure 3b, in turn, contains information about the fate of complex **11**. There is a slight polarization of the density of the

(18) r values are obtained by using the classical equation $V(r) = q\mu(\cos\theta)/r^2 - \alpha q^2/2r^4 \geq RT$ with q = 1 e, μ = 1.85 D (H_2O), and μ = 1.47 D (NH_3), $\cos\theta$ = 1, α = 0.79 Å^3, and T = 300 K. See Hirschfelder, J. O.; Curtiss, C. F.; Bird, R. B. "Molecular Theory of Gases and Liquids"; Wiley: New York, 1954.

(19) (a) Bader, R. F. W.; Runtz, G. R. *Mol. Phys.* **1975**, *30*, 117–128. (b) Bader, R. F. W.; Nguyen-Dang, T. T. *Adv. Quantum Chem.* **1981**, *14*, 63–124.

(20) Due to the fact that the maximum of the radial distribution of a diffuse GTF is far removed from its location, a Mulliken population analysis leads to unreasonable values in the case of basis sets with flat s,p GTF's. For example, Mulliken charges suggest a large transfer of negative charge from H^- to AH_n.

(21) Kraka, E.; Cremer, D. to be submitted for publication.

(22) The procomplex consists of the *noninteracting* complex partners (ion and neutral) kept at the geometry of the complex.

TABLE VI: Experimental Solvation Enthalpies of Some Anions[a]

neutral	anion		
	Cl^-	F^-	OH^-
FH	21.8	38.5	44
OH_2	14.4	23.3	22.5
NH_3	10.5	12.8[b]	

[a] Values (in kcal/mol) from ref 24–27. The PA values of the anions are 333 (Cl^-), 371 (F^-), 391 (OH^-), and 400 kcal/mol (H^-).[33] [b] Estimated from differences in binding enthalpies between $C_6H_5OH{\cdot}F^-$ (41.3), $CF_3CH_2OH{\cdot}F^-$ (39.1), and $OH_2{\cdot}F^-$ and the binding enthalpies found for $C_6H_5NH_2{\cdot}F^-$ (31.2) and $CF_3CH_2NH_2{\cdot}F^-$ (28.1 kcal/mol).[26]

OH^- ion equivalent to a charge transfer from H^3 toward O. This leads to a higher total density in the region of the electron lone pair pointing at H_2. The H_2 molecule is strongly polarized. A considerable amount of electron density is shifted from H^2 toward H^1. Again, the calculated difference density reveals that the neutral (H_2) will undergo heterolytic bond cleavage under the impact of an approaching OH^- ion.

Analysis of the Laplace concentration of $\rho(\mathbf{r})$, $\nabla^2\rho(\mathbf{r})$,[23] provides further insight into the electronic structure of ion–neutral complexes **7** and **11**. Molecular regions where the electron density concentrates more in the complex than in the procomplex are indicated by negative values of $\Delta(\nabla^2\rho(\mathbf{r}))$ (dashed contours in parts c and d of Figure 3); those where electron density concentrates less possess positive values of $\Delta(\nabla^2\rho(\mathbf{r}))$ (solid contours in parts c and d of Figure 3). The contour line maps in parts c and d of Figure 3 clearly show the development of a new O lone pair in **7** and the polarization of this lone pair toward H_2 in **11**. They also reveal that the concentration of charge at H^1 and in the nonbonding area of the O atom of **7** is partially due to a depletion of electron density in regions further remote from the nuclei of complex **7**. Obviously, electron density at the H^- ion becomes less diffuse if solvation by H_2O takes place. A similar contraction of charge can be found for H^1 in complex **11**.

Qualitatively similar difference maps of $\rho(\mathbf{r})$ and $\nabla^2\rho(\mathbf{r})$ are obtained for complexes I and II with A = F, N, or C, only that the degree of charge polarization decreases in the series **6–9** and **10–13** which can be quantitatively determined by the calculated atomic multipole moments.[21] We conclude that the binding energies of type I and type II complexes are dominated by attractive electrostatic forces resulting from charge polarization. Polarization of the electron density of an AH bond by H^- increases with the acidity of AH_n which in turn is proportional to the electron-acceptor ability of A. Polarization of the electron density of a H_2 molecule increases with the amount of electron charge located at A in AH_{n-1}^-. The actual binding energies ΔE_I and ΔE_{II} are essentially a result of electrostatic attraction and overlap repulsion.

IV. Chemical Relevance of Results

As discussed in section II, the two sets of energy data shown in Table IV provide upper and lower bounds to the true stabilities of **6–13**. The question which of these two sets of data has to be given more weight can be answered by comparing calculated solvation energies ΔE_I of H^- with the corresponding values of other ions[24–27] (Table VI). Since solvation energies should depend on both the basicity of the anion and the acidity of the neutral,[24] one can expect ΔE_I values of H^- somewhat larger than those of F^- and OH^- ions. Despite the lack of diffuse sp GTF's, HF/6-31G* energies fulfill this requirement. This is in line with similar observations made by Diercksen and Kraemer[28] who also obtained

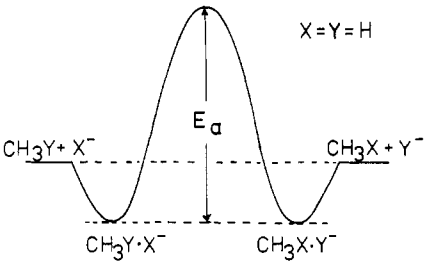

Figure 4. Energy profile of S_N2 reaction 3 for A = C.

reasonable ΔE_I values for $F^-{\cdot}H_2O$ and $OH^-{\cdot}H_2O$ with normal DZ+P basis sets at the HF level.

As for ΔE_{II}, binding energies ranging from 4 to 10 kcal/mol have been found for a variety of ion–H_2 complexes in the gas phase.[25] Again, HF/6-31G* values seem to be closer to true ΔE_{II}, values while the MP2/6-31++G** results are far too low. In view of these trends the true energy parameters of the proton-transfer reaction 2 should be close to the estimates given in Table IV. They have been obtained by reducing the HF/6-31G* values of ΔE_I and ΔE_{II} by one third of their difference to MP2/6-31++G** values and by adjusting ΔE_{II-I} to experimental ΔH_R differences.

In the case of A = O theoretical ΔE values of I and II can be compared with estimates of solvation enthalpies published by DePuy and co-workers.[29] These authors have calculated binding enthalpies of $DO^-{\cdot}H_2$ and $DOH{\cdot}H^-$ using the classical equation for the interaction potential between an ion and a neutral and calibrating the results with known solvation enthalpies. In this way, they have obtained ΔH_I and ΔH_{II} values of 24 and 7 kcal/mol for **7** and **11** and a difference ΔH_{II-I} of 7 kcal/mol, all values being within 1–2 kcal/mol of the estimated ΔE values of Table IV. Hence, it seems reasonable to base the following discussion on these results.

Ion–molecule complexes have to possess lifetimes larger than 10^{-6} s in order to be detected at room temperature by Fourier transform ion cyclotron resonance spectrometry. If we assume that dissociation of complexes I or II involves an increase in entropy by 10–20 cal/(mol K),[24,25,27] then solvated H^- ions **6–9** have to be locked in energy wells which are at least 12–15 kcal/mol below the most favorable dissociation channel. Clearly, this is not the case for CH_5^- complex **9** but holds for **6**, **7**, and **8**. We conclude that NH_4^- and OH_3^- ions **7** and **8** are stable on the time scale of the ion cyclotron resonance spectrometer experiments leading to the AH_{n+1}^- mass peaks found by Nibbering and co-workers.[1-3] In addition, we predict that FH_2^- should also be a stable species possessing probably peculiar structural features. According to our calculations, **6** and **10** have comparable energies with only an energy hump separating them. Therefore, FH^{2-} may be best considered as a F^- and an H^- ion held together by a rapidly oscillating proton. Similar to OH_3^-, FH_2^- dissociates to H_2 and AH_{n-1}^- while NH_4 dissociates to NH_3 and H^-.

Apart from stability considerations the calculated energy and structural data provide further interesting insights of chemical relevance. For example, in the gas phase CH_5^- complexes **9**, **25**, and **27** can be precursors to the transition-state **31** of the S_N2 reaction 3. This means that its intrinsic barrier is about 60 kcal/mol rather than the 55 kcal/mol calculated (Table V). Furthermore, the energy profile of a S_N2 reaction occurring in the gas phase is of the general form shown in Figure 4. For anions other than H^-, this has been amply documented by both experimental and theoretical investigations.[30,31]

(23) (a) Bader, R. F. W.; MacDougall, P. J., Lau, C. D. H. *J. Am. Chem. Soc.* **1984**, *106*, 1594–1605. (b) Cremer, D.; Kraka, E. *Angew. Chem., Int. Ed. Engl.* **1984**, *23*, 627–628. (c) Cremer, D.; Kraka, E. *Croat. Chem. Acta* **1984**, *57*, 1265–1287.
(24) Yamdagni, R.; Kebarle, P. *J. Am. Chem. Soc.* **1971**, *93*, 7139–7143.
(25) Kebarle, P. *Annu. Rev. Phys. Chem.* **1977**, *28*, 445–476.
(26) Larson, J. W.; McMahon, T. B. *J. Am. Chem. Soc.* **1983**, *105*, 2944–2950.
(27) Larson, J. W.; McMahon, T. B. *J. Am. Chem. Soc.* **1984**, *106*, 517–521.
(28) (a) Diercksen, G. H. F.; Kraemer, W. P. *Chem. Phys. Lett.* **1970**, *5*, 570–572. (b) Kraemer, W. P.; Diercksen, G. H. F. *Theor. Chim. Acta* **1972**, *23*, 398–403. (c) For a related investigation, see Kistenmacher, H.; Popkie, H.; Clementi, E. *J. Chem. Phys.* **1973**, *58*, 5627–5638.
(29) Grabowski, J. J.; DePuy, C. H.; Bierbaum, V. M. *J. Am. Chem. Soc.* **1983**, *105*, 2565–2571.
(30) See, for example: (a) Caldwell, G.; Magnera, T. F.; Kebarle, P. *J. Am. Chem. Soc.* **1984**, *106*, 959–966. (b) Pellerite, M. J., Brauman, J. I. *J. Am. Chem. Soc.* **1980**, *102*, 5993–5999. (c) Asubiojo, O. I.; Brauman, J. I. *J. Am. Chem. Soc.* **1979**, *101*, 3715–3724.

TABLE VII: Heats of Formation, $\Delta H_f°(298)$, and Reaction Enthalpies, $\Delta\Delta H_f°(298)$[a]

	$\Delta H_f°$			$\Delta\Delta H_f°$	
A	AH_n	AH_{n-1}^-	AH_{n+1}^-	(4)	(1)
C	−17.9	31.5	9	−14.6	−23
N	−11.0	25.4	7	−1.6	−18
O	−57.8	−34.2	−50	11.2	−16
F	−64.8	−60.7	−74	30.7	−13

[a] All values in kcal/mol. $\Delta H_f°(H^+)$ = 367.2; $\Delta H_f°(CHO^-)$ = 8.9 kcal/mol derived from PA(CHO^-) = 402 kcal/mol.[34]

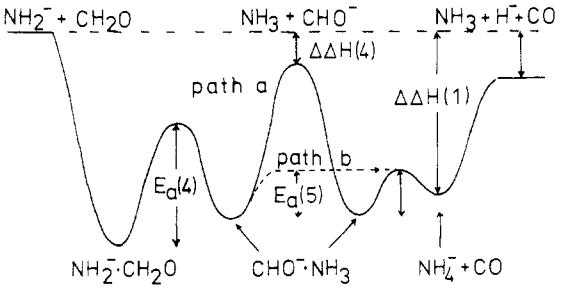

Figure 5. Energy profile of reaction 1 for A = N.

Generation of stable AH_{n+1}^- complexes by collision of AH_n and H^- is not possible under the experimental conditions of an ion cyclotron resonance spectrometer since these processes lead to considerable excess energies which cannot be dissipated by collisions with other molecules. Accordingly, AH_{n+1}^- complexes will immediately decompose. If, however, the formation of ions AH_{n+1}^- occurs as in reaction 1 via a collision complex $AH_{n-1}^-·CH_2O$, then the collision partner can carry away most of the excess energy, thus yielding stable AH_{n+1}^- complexes.[1-3] In order to clarify whether FH_2^- can be generated in the same way as OH_3^- and NH_4^-, we will briefly discuss the energy profile of reaction 1. For this purpose, we have estimated $\Delta H_f°(AH_{n+1}^-)$ from estimated ΔE_I values and have used these data in conjunction with known $\Delta H_f°$ values of AH_n, AH_{n-1}^-, CH_2O, CHO^-, and CO (Table VI).[16,32-34] In this way we have obtained the enthalpies of the reactions

$$AH_{n-1}^- + CH_2O \rightarrow AH_n + CHO^- \quad (4)$$

$$AH_n + CHO^- \rightarrow AH_{n+1}^- + CO \quad (5)$$

$\Delta\Delta H(4)$ and $\Delta\Delta H(5)$, which yield $\Delta\Delta H(1)$, the reaction enthalpy of (1) (see Table VII). A qualitative representation of the energy profile of the formation of NH_4^- via reaction 1 is shown in Figure 5.

Since reaction 4 is exothermic for A = N, generation of NH_4^- can occur via either path a or b shown in Figure 5. Experimentally, it is found that path a is preferred.[3] In case of A = O only path b is possible because of $\Delta\Delta H(4) > 0$. Accordingly, CHO^- ions can only be observed when generating NH_4^-.[1-3] NH_4^-/CO and OH_3^-/CO are formed with excess energies of 16–18 kcal/mol, which have to be partially absorbed by CO to make detection of AH_{n+1}^- ions possible.

In the case of A = C, proton transfer from CH_2O to CH_3^- is exothermic by 15 kcal/mol. Only a part of this excess energy (~5 kcal/mol[34]) is necessary to have CHO^- decompose to CO + H^- ($\Delta\Delta H$ = −2 kcal/mol), a reaction which is not possible for the other systems considered because of $\Delta\Delta H(4) \geq 0$ (Table VII). Alternatively, CH_5^- is formed via path b as a short-lived intermediate which decomposes immediately due to its relatively low stability of 6 kcal/mol.

In the case of A = F one might argue that the difference in acidities of HF and CH_2O is far too large and, hence, reaction 4 far too endothermic (31 kcal/mol, Table VII) to permit formation of the complex HF·CHO^-. If, however, this complex is stable by at least 36 kcal/mol relative to HF and CHO^-, then its formation would be exothermic by an energy amount (~5 kcal/mol) probably sufficient to allow hydride transfer and the formation of FH_2^- via path b. HF solvation energies of anions range from 20 ($HF·Cl^-$[27]) to 40 kcal/mol ($HF·H^-$, Table IV). Accordingly, there is a limited chance that FH_2^- can be observed as a collision product of F^- and CH_2O in the ion cyclotron resonance spectrometer.

Note Added in Proof. After this work had been finished Prof. P. v. R. Schleyer brought to our attention that he and his coworkers have also performed HF and MP calculations on NH_4^-.[35] Their results are in accord with ours. Prof. H. Budzikiewicz informed us of the detection of a spurious CH_5^- ion in a quadrupole mass spectrometer set up for negative chemical ionization.[36] Our theoretical results helped to identify the "pseudonegative" ion as CH_5^+.

Acknowledgment. It is a pleasure to acknowledge fruitful discussions with Prof. H. Budzikiewicz. This work was supported by the Deutsche Forschungsgemeinschaft and the Fonds der Chemischen Industrie. All calculations have been carried out at the Rechenzentrum der Universität Köln.

Registry No. H_2, 1333-74-0; OH_3^-, 12325-19-8; NH_4^-, 12325-21-2; CH_5^-, 12316-54-0; H^-, 12184-88-2; F^-, 16984-48-8.

(31) (a) Schlegel, H. B.; Mislow, K.; Bernardi, F.; Bottoni, A. *Theor. Chim. Acta* **1977**, *44*, 245–256. (b) Wolfe, S.; Mitchell, D. J.; Schlegel, H. B. *J. Am. Chem. Soc.* **1981**, *103*, 7692–7694, 7694–7696.

(32) Cox, J. D.; Pilcher, G. "Thermochemistry of Organic and Organometallic Compounds"; Academic Press: London, 1970.

(33) (a) Bartmess, J. E.; Scott, J. A.; McIver, Jr., R. T. *J. Am. Chem. Soc.* **1979**, *101*, 6046–6056, 6056–6063. (b) Bartmess, J. E.; McIver, Jr., R. T. In "Gas Phase Ion Chemistry", Vol. 2, Bowers, M. T., Ed.; Academic Press: New York, 1979; pp 87–121.

(34) Chandrasekhar, J.; Andrade, J. G.; Schleyer, P. v. R. *J. Am. Chem. Soc.* **1981**, *103*, 5612–5614.

(35) Kos,. A. J.; Schleyer, P. v. R.; Pople, J. A.; Squires, to be submitted for publication.

(36) Poppe, A.; Schröder, E.; Budzikiewicz, H., to be submitted for publication.